Analyst

PAPER

Mesoporous titania thin films as efficient enzyme carriers for paraoxon determination/detoxification: effects of enzyme binding and pore hierarchy on the biocatalyst activity and reusability

Cite this: DOI: 10.1039/c4an00152d

N. Frančič,[a] M. G. Bellino,[b] G. J. A. A. Soler-Illia[b] and A. Lobnik*[a]

Received 21st January 2014
Accepted 22nd January 2014

DOI: 10.1039/c4an00152d

www.rsc.org/analyst

In this work we demonstrate the efficient immobilization of histidine 6-tagged organophosphate hydrolase (His_6–OPH), an organophosphate-degrading enzyme, on mesoporous titania thin films. This permits the use of the biocatalyst films as efficient tools in the detection/detoxification of paraoxon. His_6–OPH was immobilized on mesoporous thin films with uniform (9 nm) and bimodal (13–38 nm) pore size distribution, through covalent attachment and physical adsorption. The biocatalyst films show good activity, and enhanced stability with respect to the free enzyme at extreme conditions of pH and temperature, especially around neutral pH and room temperature. In addition, the bioactive films can be easily separated from the reaction media and reused multiple times without significant loss of activity.

Introduction

The utilization of enzymes as biocatalysts has become an important avenue in chemical and pharmaceutical industries for preparing biochemical products, biosensors and drugs.[1–5] However, most native enzymes exhibit high reactivity and selectivity in solution under relatively mild conditions, *i.e.*, near neutral pH and at 25–40 °C. Under extreme conditions, enzymes are easily inactivated due to denaturation, either by changes in conformation or other transformations of stereo chemical structure. Thus, native enzymes often suffer severe limitations in broader applications. Moreover, the utilization of natural enzymes has other processing difficulties such as the reuse of enzymes, product contamination, and separation. One of the approaches for resolving these difficulties is to immobilize enzymes on solid surfaces thus producing recoverable and stable heterogeneous biocatalysts.[6–12]

Organophosphorus hydrolase (OPH, EC 3.1.8.1) is a 72 kDa homodimeric metalloenzyme capable of hydrolyzing a broad spectrum of organophosphorous compounds (OPCs), pesticides (*e.g.* paraoxon, parathion, *etc.*) and warfare agents (*e.g.* sarin, soman, and VX), by producing less toxic products, such as *p*-nitrophenol in the case of paraoxon and parathion.[13] OPH is one of the most studied enzymes related to its activity towards pesticides and nerve agents. OPH catalyzes hydrolysis reactions of various organophosphorus compounds containing P–O, P–F, and P–S bonds.[14] Fusing a hexahistidine (His_6) tag to OPH changed enzyme's catalytic and physical chemical properties,[15] improved its catalytic efficiency, especially towards P–S containing substrates, and its stability under alkaline hydrolysis conditions compared to native OPH.

A number of approaches have been presented for the immobilization, encapsulation, and entrapment of OPH with the aim of creating materials with preserved organophosphate hydrolase activity. OPH has been immobilized onto various organic[16–21] as well as inorganic materials;[22–32] a common inorganic material used for OPH immobilization and entrapment is silica, where encapsulation[23,24,27–29] and covalent immobilization strategies[25,26] have been reported for sol–gel matrices. Both, covalent and non-covalent immobilization techniques, as well as entrapping OPH into sol–gel materials, yield materials retaining relatively good enzyme activity. Furthermore, immobilization offers increased storage, temperature, and pH stability of the immobilized enzyme. However, there are some limitations including decreased activity, which is due to the possible irreversible damage to the enzyme during the immobilization step, and slow response rate to selected substrates. To overcome the drawbacks of modification of OPH during the encapsulation or covalent immobilization step, materials have been created with non-covalent decoration of OPH. Lei *et al.* have developed functionalized mesoporous silica and utilized nonspecific, ionic interactions for OPH binding, resulting in a material possessing stabilized enzyme with greater activity compared with an ordinary porous material. Compared with normal porous materials this one exhibits increased activity, high immobilization efficiency and enzyme stability due to the

[a]*Centre of Sensor Technology, Faculty of Mechanical Engineering, University of Maribor, Smetanova 17, 2000 Maribor, Slovenia. E-mail: aleksandra.lobnik@um.si; Fax: +386-2-333-56-80; Tel: +386-2-333-56-64*

[b]*Gerencia Química, Centro Atómico Constituyentes, Comisión Nacional de Energía Atómica, Avenida General Paz 1499, 1650 San Martín, Provincia de Buenos Aires, Argentina*

high surface area and increased matrix pore size.[30–32] While this study demonstrated that a controlled surface charge is relevant to the enzyme incorporation, some limitations remain. For example, the bio-material was prepared and tested at a pH of 7.5; however, no behaviour at different pHs was observed, where the surface charges of the supporting material and the enzyme change. In addition, it is known that OPH is more efficient at pH > 9.0.[13] Higher pH values also raise the question of the suitability of chosen material, namely silica is not resistant to it and therefore, probably not the best choice for sensor preparation. This is a reason to explore other mesoporous frameworks that are known to be resistant to high pH conditions.

Mesoporous materials present a wide range of highly controlled pore sizes and shapes, which have been proven to be useful for enzyme trapping. Enzyme immobilization on inorganic mesoporous materials is an interesting method for improving enzyme functionality.[33–36] Porous materials have large specific surface areas, as well as high mechanical, thermal, and chemical stabilities. Due to their high surface area and large pore sizes, mesoporous materials present high adsorption and outstanding pore accessibility; pores can be designed to incorporate proteins through physical or chemical methods, thus providing active biomaterials.[18] In particular, applications of TiO_2 mesoporous matrices as enzyme carriers have aroused increasing interest in recent years. Due to its good biocompatibility, environmentally benign nature, and chemical and thermal stabilities, TiO_2 is a potential material for the immobilization of enzymes.[37–46] Furthermore, a titania matrix is resistant to high pH values, *i.e.* pH > 9 where OPH is more efficient. Despite most of them being able to accommodate large enzymes,[47,48] no attempt at the hydrolysis of organophosphates with enzyme-loaded mesoporous TiO_2 materials has yet been reported. Mesoporous thin films are particularly interesting because they are amenable to integration within devices that display properties derived from pore architecture and pore functionalization,[49,50] and their use can be extended to micro- and nanofluidics. Naturally, pore sizes and inter-pore necks must be adequately tailored to accommodate large biomacromolecules, such as His_6–OPH.[15] Recently, it has been shown that titania thin films, with tuned hierarchical pore-size distributions and pores ranging between 10 and 200 nm, could indeed be manufactured[51] and used for enzyme immobilization.[52] The possibilities to conjugate biomolecules onto mesoporous titania thin films are numerous, and rely on two main strategies: adsorption and post-synthetic functionalization of the prepared material, which enables covalent attachment of biomolecules. Publications employing enzyme/peptide immobilization have employed the adsorption mechanism for the selected enzyme[52] and silanization for introducing ideal anchorages onto the surface of mesoporous thin films for covalent binding of specific molecules.[53] However, these methods either produce inefficient immobilization or require multiple steps that result in complicated and time-consuming procedures.

The present work describes a simple and novel strategy for the direct detection and/or detoxification of OPCs where mesoporous thin films supported on glass slides are used as efficient host matrices for active enzymes. The enzyme, His_6–OPH, was covalently attached on/into the pores of mesoporous titania films with retained catalytic activity. As a proof of concept, this work reports on the hydrolysis of organophosphate (paraoxon) by His_6–OPH functional mesoporous bio-catalyst films. We show here that these bio-catalysts are easy to prepare, easy to separate from the reaction mixture, and can be reused several times without significant losses in hydrolytic activity.

Experimental

Materials and methods

Materials. $TiCl_4$ (99.9%), triblock-copolymer Pluronics F127 (PEO_{106}–PPO_{70}–PEO_{106}), poly(propylene glycol) PPG (PPO_{68}, $M_W \approx 4000$), butanol, tetrahydrofuran (THF), 2-(cyclohexylamino) ethanesulfonic acid (CHES), 4-(2-hydroxyethyl)-1-piperazine-ethanesulfonic acid (HEPES), and cobalt chloride hexahydrate were purchased from Aldrich, and used as received.

The His_6–OPH enzyme was isolated and purified as previously described.[54] The enzyme-specific activity was 6000 U mg^{-1}.

Enzyme adsorption. Protein immobilization was achieved by immersing millimeter-sized pieces of the thus-nanoporous films (50 mm^2 total geometrical area) in 1 mL of a 0.1 mg mL^{-1} OPH (specific activity of 6000 U mg^{-1}) in buffered solution (20 mM Tris–HCl (pH 7.5); 50 mM KCl) for an appropriate time. At the end of the immobilization period (24 h), the biocatalyst films were thoroughly rinsed with water, to remove the excess of unbound His_6–OPH, dried, and kept refrigerated (4 °C) for further analysis.

Covalent attachment of the enzyme. The enzyme was covalently attached *via* reactive carbonyl groups on the titania thin films which were formed by the use of *N*,*N*′-carbonyldiimidazole (CDI), a highly reactive carboxylating agent that contains two acylimidazole leaving groups. The activating agent and the intermediate reactive group are mostly susceptible to hydrolysis, therefore, the activation was done under non-aqueous conditions.

Appropriate pieces of nanoporous thin films (50 mm^2 total geometrical area) were repeatedly washed with anhydrous THF for several times in order to eliminate any traces of water. *N*,*N*′-Carbonyldiimidazole (CDI) was then added into the 1.5 mL micro-centrifuge tube containing THF at a final concentration of 50 mg mL^{-1} and reacted at 750 rpm mixing in a shaker for 2 h at room temperature. The thin films were washed three times with THF to remove the excess CDI and any reaction by-products, and subsequently three quick washes were performed with 0.025 M CHES buffer (pH 9.3) to remove traces of THF. OPH was then dissolved in 0.025 M CHES buffer at a final concentration of 0.1 mg mL^{-1} (specific activity of 6000 U mg^{-1}), and then added to the thin films. The conjugation mixture was kept at room temperature and 750 rpm mixing in a shaker for 48 h. The amount of His_6–OPH bound onto the prepared thin films was calculated from the difference between the initial His_6–OPH added and the remaining amount of His_6–OPH in the supernatant as determined by the Bradford method. The thin films were then washed 3 times in 0.025 M CHES buffer (pH 9.3)

to remove any un-reacted OPH. The OPH conjugated thin films were stored in 0.05 M sodium phosphate buffer (pH 7.5) at 4 °C for subsequent analysis and use. The procedure for the overall functionalization of mesoporous thin films and enzyme attachment is shown in Scheme 1.

Quantitative analysis of immobilization using the Bradford method and determination of immobilization efficiency. In order to quantify enzyme immobilization, the supernatant was separated from the thin films, and the Bradford method[55] was used for protein determination in the supernatant with Coomassie Brilliant Blue G-250 reagent. The amount of immobilized protein was considered to be the difference between the total incubated amount and the protein in the supernatant.

The immobilization efficiency of the His_6–OPH enzyme onto the mesoporous TiO_2 films determined by the Bradford method used the following relationship to calculate the percentage immobilization of the enzyme.

$$\text{Immobilization percentage} = \frac{\text{Total amount of enzyme added} - \text{Free enzyme}}{\text{Total amount of enzyme added}} \times 100$$

Evaluation of enzyme activity. The enzymatic activity was determined spectrophotometrically using an Agilent 8453 UV-visible spectroscopy system with a thermostatted cell (Agilent Technology, Waldbronn, Germany). The accumulation of the *p*-nitrophenolate anion ($\lambda = 405$ nm; $\varepsilon = 17\,000\ M^{-1}\ cm^{-1}$, pH 9.0; $\varepsilon = 18\,500\ M^{-1}\ cm^{-1}$, pH 10.5) as a hydrolysis product of paraoxon was monitored. The enzyme concentration hydrolyzing 1 μmol of the substrate (paraoxon) per minute at 25 °C was considered as one unit of enzymatic activity.

The enzymatic reaction rates were calculated using the initial linear sections of the kinetic curves ($v_0 = tg\alpha$), where the increase is linear. The maximum rate of the enzymatic reaction (V_{max}) and the Michaelis constant (K_m) were determined using double reciprocal coordinated $1/v_0 - 1/[S]$ (the Lineweaver–Burk plot), in which v_0 is the initial velocity, V_{max} is the maximum velocity and $[S]$ is the concentration of the substrate.[56]

In order to investigate the influence of pH on the enzyme catalytic activity, various 50 mM buffers with overlapping pH values were used: K-phosphate, pH 6.5–8.0 and 11.0–12.0, Tris, pH 7.5–9.0, CHES, pH 8.5–10.0, Na-carbonate, pH 9.5–11.0.

The most important properties of the bio-sensing film for real applications is its reproducibility and reusability. Measurements of the reusability were performed in thermostatted vessels at a temperature of 20 °C, pH 10, and a 0.15 mM substrate (POX) concentration. Between each measurement, samples were washed with water 3-times for 5 min in closed micro-centrifuge tubes on a vortex shaker (750 rpm).

Apparatus. The pH values of all solutions were determined using a Mettler Toledo, Seven EasyTM, pH meter S20.

The ATR-FTIR spectra were recorded on a Perkin Elmer Spectrum GX spectrometer. The ATR accessory (supplied by SpecacLtd., UK) contained a diamond crystal. All spectra (16 scans at 4 cm^{-1} resolution and rationed to the appropriate background spectrum) were recorded at room temperature.

Field emission-scanning electron microscopy (FE-SEM) images were taken with a Zeiss Leo 982 Gemini electron microscope in the secondary-electron mode, using an in-lens detector to improve the resolution.

Pore- and neck-size distributions of titania films were obtained by water adsorption–desorption isotherms at 298 K. Isotherms were determined by environmental ellipsometric porosimetry (EEP) using a SOPRA GES5A apparatus, equipped with microspot optics. The film thickness and the real component of the refractive index were obtained by fitting the ellipsometric parameters $\Psi(\lambda)$ and $\Delta(\lambda)$in the 400–800 nm range;[57] the film refractive index was described according to a modified Cauchy equation. WinElli 2 software (SopraInc), which transforms the variation of n with P/P_0 into a filled pore volume by using a three-medium BEMA treatment, was used. Pore- and neck-size distributions are derived by Environmental Ellipsometric Porosimetry (EEP) according to the techniques and models reported by Boissiere *et al.*[58]

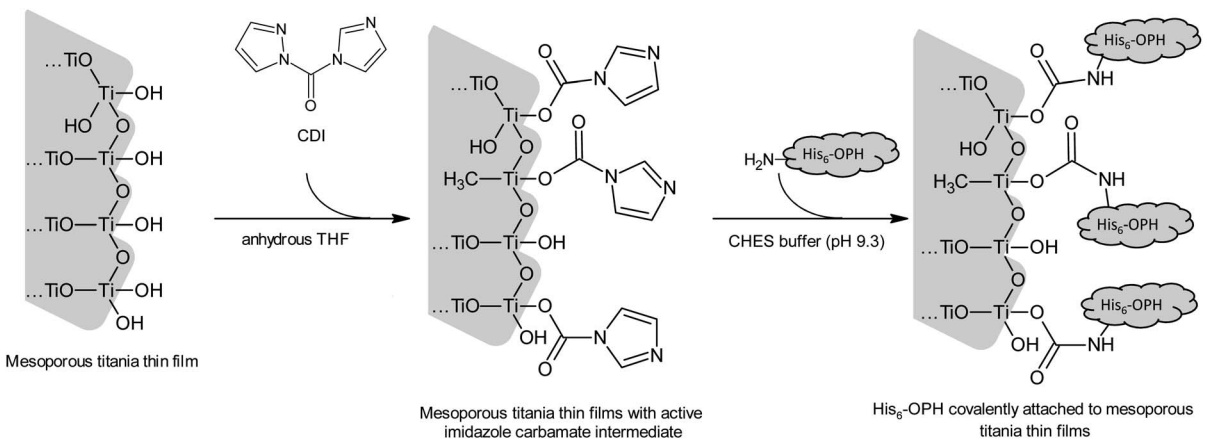

Scheme 1 Schematic representation of the preparation route of His_6–OPH–conjugated mesoporous titania thin films through the CDI mediated reaction.

Synthetic procedures

Mesoporous titania film synthesis. The supported mesoporous titania thin films with unimodal or bimodal pore size distribution were produced following a procedure reported by Malfatti *et al.*,[51] by carefully adjusting the relative proportions of the precursor ($TiCl_4$), water, template (Pluronics F127), co-template (PPG) and solvent (butanol) in the sols. Titania films were produced by dip-coating at a withdrawal rate of 0.5 mm s^{-1}. Prior to deposition, soda-lime glass slides were washed thoroughly with dextran, and rinsed successively with water, ethanol, and acetone. The relative humidity (RH) during dip-coating was set at 20%. After deposition, films were aged at 50% RH for 24 h, and then dried at 60 and 130 °C for 24 h at each temperature. Finally, they were calcined in air at 350 °C for 2 h; the temperature ramp was 1 °C min^{-1}. Molar ratios in the precursor sols were the following, $TiCl_4/BuOH/H_2O/F127/PPG = 1 : 40 : 4 \times 10^{-3} : P$, where $P = [PPG]/[Ti]$, was 0 and 6.2×10^{-3} for conventional and bimodal mesoporous films, respectively. The resulting films were characterized as described in the Apparatus section (FE-SEM and EEP).

Results and discussion

Titania films characterization

To investigate the influence of enzyme carrier on biocatalyst performance, we prepared films with uniform pore-size distribution and 9 nm diameter mesopores. The porosity of these films should be the limiting step in the successful incorporation of the enzyme in mesopores; OPH can be described as an elongated molecule, with 9 nm in the longest axis, and 4 nm shorter diameter.[59] Larger mesopores could potentially accommodate enzymes and shield the immobilized enzyme from external influences (*e.g.* pH, temperature).

Fig. 1 shows the nanoporous structure of the titania films obtained, including monodisperse or hierarchically mesoporous films with larger mesopores. Transparent, crack-free mesoporous thin films are obtained after the deposition-calcination steps. FE-SEM micrographs of typical mesoporous titania thin films obtained under our synthesis conditions are displayed in Fig. 1A and C. Depending on the initial sol composition the prepared films exhibit a uniform 9 nm diameter or hierarchical pore-size distributions of 13 and 38 nm, according to SEM. These films are labelled as TiF-9 and TiF-13/38 according to the size of their pores. EEP was used to measure water adsorption–desorption isotherms, from which the pore volume and pore size were derived. Measurements on titania films are presented in Fig. 1B and D. The films present a high porous volume (30 to 40% pore volume) and a very well defined pore size distribution, which were in excellent agreement with the SEM measurements. The textural characteristics of these films are summarized in Table 1.

ATR-FTIR characterization of biocatalyst films

To confirm the successful immobilization of His_6–OPH on hierarchical mesoporous titania thin films, ATR-FTIR spectra were recorded (Fig. 2). The FTIR spectra in the 4000–650 cm^{-1} region show the characteristic bands of the inorganic framework and the organic functions incorporated in the mesoporous samples. The ATR-FTIR spectra of the bare mesoporous titania thin film (solid line) showed a weak and large band peaking around 3250 cm^{-1} which is assigned to O–H stretching mode, due to Ti–OH species and adsorbed water.[60] Small signals for

Table 1 Textural characteristics determined by FE-SEM images and EEP (environmental ellipsometric porosimetry) of the resulting mesoporous films

	TiF-9	TiF-13/38
Mean pore size (nm)	8.6	13 and 38
Film porosity (%)	38	47
Film thickness (nm)	68	78

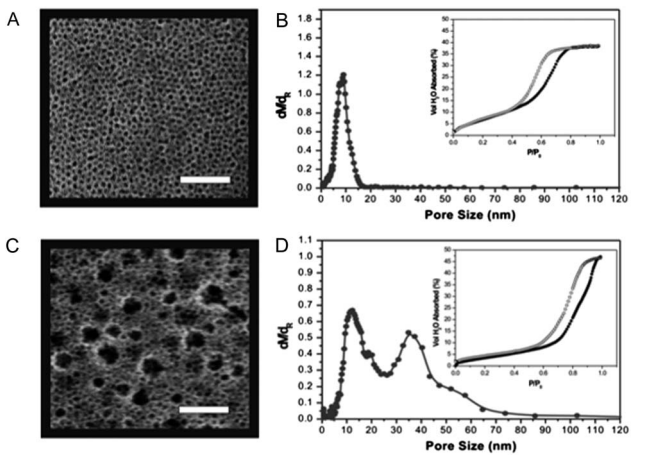

Fig. 1 FE-SEM images (A and C), pore-size distribution (B and D) and water adsorption–desorption isotherms (B and D, insets) of the titania thin films: TiF-9 (upper frame), and TF-13/38 (lower frame); scale bar = 100 nm.

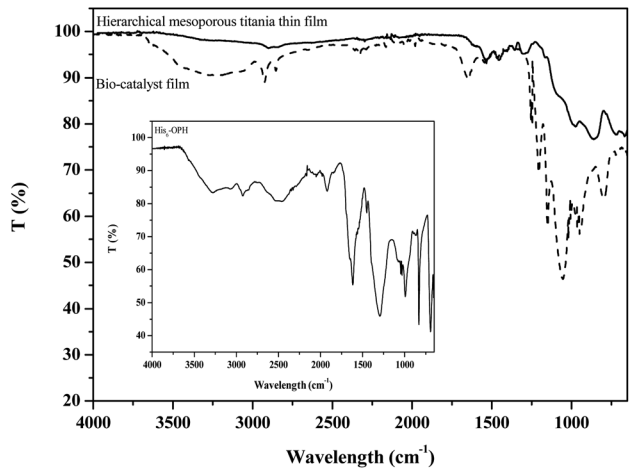

Fig. 2 The ATR-FTIR spectra of a hierarchical mesoporous titania thin film (solid line) and the same film containing His_6–OPH (dashed line). The inset shows the FTIR signature of the enzyme.

traces of the organic template (surfactant) are indicated by the C–H stretching bands around 2900 cm^{-1}.[61] The bands between 600 and 800 $cm^{-1}$are typical of the formation of Ti–O and Ti–O–Ti bonds.

Considerable modification of the IR spectra regarding the biocatalyst films (dashed line) can be seen due to immobilization. We identified new characteristic absorption bands of His_6–OPH between 1620 and 1700 cm^{-1} and within the region between 1400 and 1200 cm^{-1} as well as some shifted bands corresponding to the support (600–800 cm^{-1}). The broad bands from 3000–3700 cm^{-1} were strongly influenced by immobilization; their intensity increased considerably after immobilization and this is characteristic of both free water and enzyme. Native and supported His_6–OPH signals were ascribed to the amide group and those of particular side chains of the amino acids.[62–64] The ATR-FTIR spectrum of the enzyme had a broad band in the 3000–3500 cm^{-1} region which originated from the O–H and N–H stretching vibration and could be identified as Amide A (3500 cm^{-1}) and Amide B (3100 cm^{-1}). Amide I and amide II bands are two major bands of the protein infrared spectrum. The Amide I band (1600–1700 cm^{-1}) is mainly associated with the C=O group stretching vibration in the backbone of the protein and is directly related to the protein conformation. The signals in the 1510 and 1580 cm^{-1} region were assigned to the symmetrical bending of the N–H bonds corresponding to the NH^{3+} group of the amino acids, which are characteristic of the Amide II region. Similarly, the N–H bond showed stretching vibrations at 3310 and 3450 cm^{-1} of the characteristic Amide A region. Amide III bands are very complex bands found in the region between 1400 and 1200 cm^{-1} and are very dependent on the force field, the nature of side chains and hydrogen bonding.[62–64]

Immobilization efficiency and kinetic studies

Direct determination of the amount of His_6–OPH adsorbed and covalently attached to the films presents some difficulties due to the very low quantities of the film (*ca*. 1 mg cm^{-1}) and enzyme. However, enzyme loading in the film was determined from the difference of enzyme concentration in solution before and after the immobilization step by the Bradford method (Table 2). While physical adsorption leads to enzyme loading below 20%, enzyme incorporation efficiencies between 45 and 65% were reached for films with covalently bonded enzymes. Comparing the immobilization efficiencies to other materials[25,27,29] the resulting effect is lower; however, advantages of the present biocatalyst are discussed further on. The quantity of covalently attached His_6–OPH in 50 mm^2 area of mesoporous thin films was estimated to be about 44 μg for TiF-9 biocatalyst films and around 60 μg for biocatalyst films with bimodal pore size distributions (TiF-13/38). As a comparison of both immobilization strategies, the quantities of adsorbed enzyme on mesoporous films were 15 μg for the TiF-9 biocatalyst film and around 20 μg for the bimodal mesoporous biocatalyst film. As a first conclusion, the immobilization efficiency in mesoporous thin films with chemically modified surface was higher than the one corresponding to simple enzyme adsorption.

As shown in Table 2, covalent attachment of His_6–OPH leads to higher protein uptakes; in particular, the highest enzyme loadings were obtained on bimodal mesoporous thin films. Although the necessary conditions to perform covalent attachment of an enzyme to a carrier were such (pH 9.3 and 24 h stirring at RT) that some loss of activity is inevitable, enzyme immobilization by chemical binding provides numerous advantages; one of them being limited leakage or detachment of an enzyme. Namely, because of the stable nature of the bonds formed between the enzyme and matrix, the enzyme is not released into the solution upon use. Furthermore, other advantages are easy accessibility of the immobilized enzyme by the substrate and increased pH as well as temperature stability due to strong interactions between the enzyme and the support material.[65]

Table 2 His_6–OPH immobilization efficiencies and activities

Sample/type of immobilization	Immobilization efficiency (%)	Activity (U mm^{-2} carrier)
TiF-9 cov.	44.1 ± 2.3	5.3 ± 0.1
TiF-13/38 cov.	65.5 ± 2.0	7.8 ± 0.3
TiF-9 ads.	15.2 ± 1.0	1.8 ± 0.2
TiF-13/38 ads.	18.4 ± 2.1	2.2 ± 0.1

Performance, stability, and reuse of synthesized biocatalyst films

The bio-functionalized mesoporous films show a significant ability to hydrolyze paraoxon when immersed in paraoxon solution (Fig. 3). Blank experiments performed on mesoporous titania films without the enzyme showed no catalytic activity. These results demonstrate that the used mesoporous materials lead to the successful covalent or physical attachment of a large

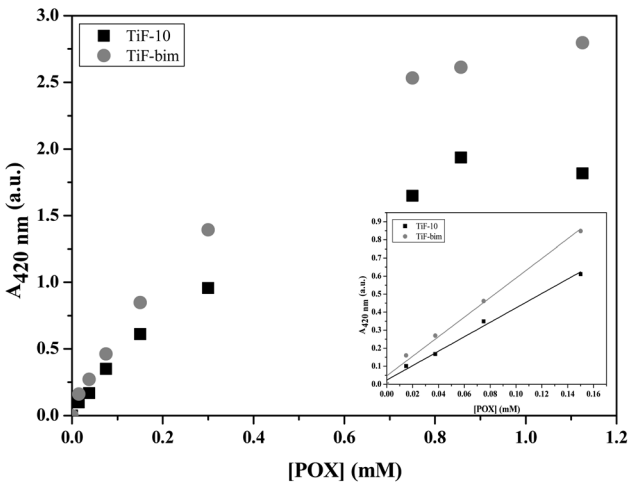

Fig. 3 Hydrolysis of paraoxon with covalently attached His_6–OPH biocatalyst films TiF-10 and TiF-bim measured at $A = 420$ nm after 5 min. Inset, biocatalyst films detection linear range. Measurements were performed with selected 50 mm^2 bio-functionalized mesoporous titania thin-films with covalently attached His_6–OPH at 20 °C, pH 10.5 (CB, 50 mM), and different substrate concentrations.

quantity of enzyme molecules that preserve their catalytic properties, even after some enzyme loss as discussed above.

Determination of the kinetic parameters for paraoxon hydrolysis by free and immobilized His_6–OPH demonstrated that depending on the immobilization method (covalent attachment *vs.* physical adsorption) and mesoporosity (TiF-9 and TiF-13/38) the catalytic efficiency (k_{cat}/K_M) of an immobilized enzyme was approximately 40–400 times lower than the free enzyme, primarily due to a decrease in turnover number (k_{cat}). When an enzyme was immobilized, regardless of the immobilization type or porosity, the K_M of the immobilized enzyme increased (approx. 10–50 times) while the V_{max} decreased (approx. 15–40 times); meaning that the affinity of the enzyme for its substrate and the velocity of enzymatic reaction decreased. The enzyme immobilized by covalent attachment displayed "worse" results than those of the adsorbed enzyme, which is understandable, namely, covalent bonding involved exposure of the enzyme to a harsher environment (pH 9.3) and toxic reagents (THF, CDI). However, covalent bonding offers other advantages, the most important being elution of the enzyme into the reaction mixture and its reusability.

The important issue in designing a bio-catalyst for the use in bio-sensors' is diffusional resistance offered to the substrate. This can be evaluated by comparing apparent K_M values for free and immobilized enzymes, where K_M for the immobilized enzyme is strongly dependent on the diffusional resistance. Typically, the differences in K_M for free and immobilized enzymes are due to their steric effects, ionic and strength diffusional limitations, as the porous material possesses an additional mass transfer resistance resulting in diffusion from bulk solution through the pores. The change in affinity of the enzyme to the substrate probably resulted from structural changes in the enzyme introduced by the immobilization procedure or by lower accessibility of the substrate to the active site of the immobilized enzyme. For comparison of the effect of mesoporosity on the catalytic performance, two types of prepared biocatalyst films with covalently attached enzyme were used, one being the film with uniform pore size distribution (TiF-9) and second, the film with hierarchical pore size distribution (TiF-13/38). Kinetic parameters were determined using Michaelis–Menten and Lineweaver–Burk plots. As expected, the K_M of an immobilized enzyme is higher than the one of the enzyme in solution (Table 3), where K_M and V_{max} were found to be (0.48 ± 0.02) mM and $(43 \pm 0.2) \times 10^{-3}$ mM s^{-1} for TiF-9, and 0.98 ± 0.07 mM and $(98 \pm 0.1) \times 10^{-3}$ mM s^{-1} for TiF-13/38, respectively.

As mentioned before, for both samples the K_M increased and V_{max} decreased, where TiF-9 exhibited smaller changes ($\sim$17 times increase of K_M and $\sim$50 times decrease of V_{max}) in comparison to the free enzyme. Thanking the immobilization efficiency (44 and 65%), the catalytic efficiency of both samples is approximately the same (Table 3). In addition to provide an efficient platform for pesticide degradation, the biocatalyst films presented here permit the assessment of paraoxon (POX) concentration. The accumulation of a hydrolysis product, *p*-nitrophenol, was measured spectrophotometrically at 420 nm. A linear increase in *p*-nitrophenol was observed after the 5 min reaction of POX with biocatalyst films; the optimum concentration range for determination is from approximately 0.035 to 0.8 mM (Fig. 3). The lowest concentration of POX measured with the available spectrophotometer for both biocatalyst films was determined at approximately 15 μM ($\sim$4.1 mg L^{-1}). Hydrolysis of POX was even more visible and easier to detect with TiF-bim biocatalyst (Fig. 3).

The limit of detection (LOD) of these biocatalyst films is approximately 5 times less than the value obtained with the silica based biocatalyst published in our previous work (80 μM),[29] and up to our knowledge, the lowest LOD for the selected analyte, paraoxon, was measured optically by absorbance spectrometry. The majority of papers is focused on electrochemical detection,[26,30] where detection limits are understandably lower. However, it must be kept in mind that the enzyme-mesoporous platform presented here also permits the production of electrochemically active materials through film deposition onto a conductive substrate. Current results show an improvement in lowering the LOD for paraoxon sensing, and the reached detection limit is in the range of the lethal dosage level (7 μM in rats and mice). As presented, though, our biocatalyst films still do not reach the EU Water Framework Directive aims for the assessment, monitoring and management of water quality in rivers, lakes, groundwater, and coastal beaches. This directive establishes that individual pesticides and their transformation products should be monitored at the 0.1 μg L^{-1} level and the total pesticide concentration cannot exceed 0.5 μg L^{-1}.[66] The biocatalyst films presented here exceed this value for approximately three orders of magnitude. However, the main limitation lies in the existing detection technique, which could probably be improved, and in the sensitivity of developed biocatalyst films.

In order to be able to incorporate the biocatalysts for various advanced applications, it is desirable to enhance their stability in harsh environmental conditions, such as pH and temperature. As it is known, for most enzymes the catalytic activity is strongly dependent on the pH and *T*. Therefore, with the purpose of comparing the activities of a free and immobilized enzyme, the experimental conditions were set at 20 °C, pH 10.5 (CB 50 mM), and a POX concentration of 0.15 mM.

Table 3 Kinetic constants for POX hydrolysis by free and immobilized His_6–OPH

Sample	V_{max} (10^{-3} mM s^{-1})	K_M (mM)	k_{cat} (s^{-1})	k_{cat}/K_M (M^{-1} s^{-1})
Free enzyme – His_6–OPH[15]	2.5 ± 0.1	$(10 \pm 0.5) \times 10^{-3}$	5100 ± 100	$(5.1 \pm 0.3) \times 10^8$
Covalent attachment (TiF-9)	43 ± 0.2	0.48 ± 0.02	700 ± 10	$(1.5 \pm 0.1) \times 10^6$
Covalent attachment (TiF-13/38)	98 ± 0.1	0.98 ± 0.07	1150 ± 30	$(1.2 \pm 0.2) \times 10^6$
Physical adsorption (TiF-9)	78 ± 0.2	0.23 ± 0.02	2900 ± 45	$(1.3 \pm 0.2) \times 10^7$

The activities of the free and immobilized His_6–OPH at different pH values and temperatures are compared in Fig. 4. In both cases, the enzyme exhibited a maximum activity over a relatively wide pH range (Fig. 4a), from 10.5 to 12.0 and 10.5 to 11.0/11.5, respectively. The bound enzyme displayed a steady catalytic activity over the wide pH range from 7.5 to 11.0. The enzyme immobilization results in higher activity at lower pH values, allowing the His_6–OPH to operate with more than a 20% higher relative activity at neutral pH in comparison to the enzyme in solution. The observed trend broadened over the wide pH range until pH 9.5, where the residual activity of the bound enzyme equaled the one in solution and at pH between 11.0 and 12.0 it drops rapidly.

The temperature optimum (Fig. 4b) for both enzymes was reached between 53 and 58 °C, respectively. It is clear that the immobilization of the enzyme enhances its activity at lower temperatures. Indeed, the activity of the immobilized His_6–OPH at 25 °C was between 55 and 65%, respectively, and led to an overall 10% increase in relative activity across the broad temperature range (20 to 45 °C) in comparison with the enzyme in solution. From the practical point of view, we can conclude that the use of the present bio-catalytic film would relieve the rather stringent conditions that most processes based on free enzyme catalysis require. These findings permit the expansion of the possible uses of the bio-sensing layers significantly.

The immobilization stability of an enzyme can be determined from the number of possible re-cycles. The covalently immobilized His_6–OPH retained its activity in alkaline pH = 10.5 with practically no significant loss even after the reaction was repeated eight times (Fig. 5), indicating excellent performance of the TiF-bound enzyme.

The reuse of enzymes in multiple reaction cycles is one of the main objectives of immobilization. This is very important from the point of view of reducing the cost of the enzyme, which is an important factor while considering its suitability for commercial applications, and is particularly important for highly priced enzymes. Usually, it is considered that an enzyme can be reused until its activity decreases to less than 25% from the initial value.[67]

There is only a minor difference between the two types of mesoporous films used for enzyme immobilization, TiF-9 and TiF-bimodal (TiF-13/38). While the activity of covalently attached TiF-9–OPH remains fairly constant at 100% throughout the whole 8 cycles, there was a slight drop in activity, of about 20%, for TiF-bimodal-OPH. The reason for the activity drop of bimodal films may be due to enzyme adsorption into the larger pores (40–100 nm) and its subsequent detachment out of them during repeated usage. The TiF-9 films do not offer this additional "hiding within the pores", because the OPH is larger than synthesized pores. As a comparison, the reusability of mesoporous titania thin films, with adsorbed enzyme

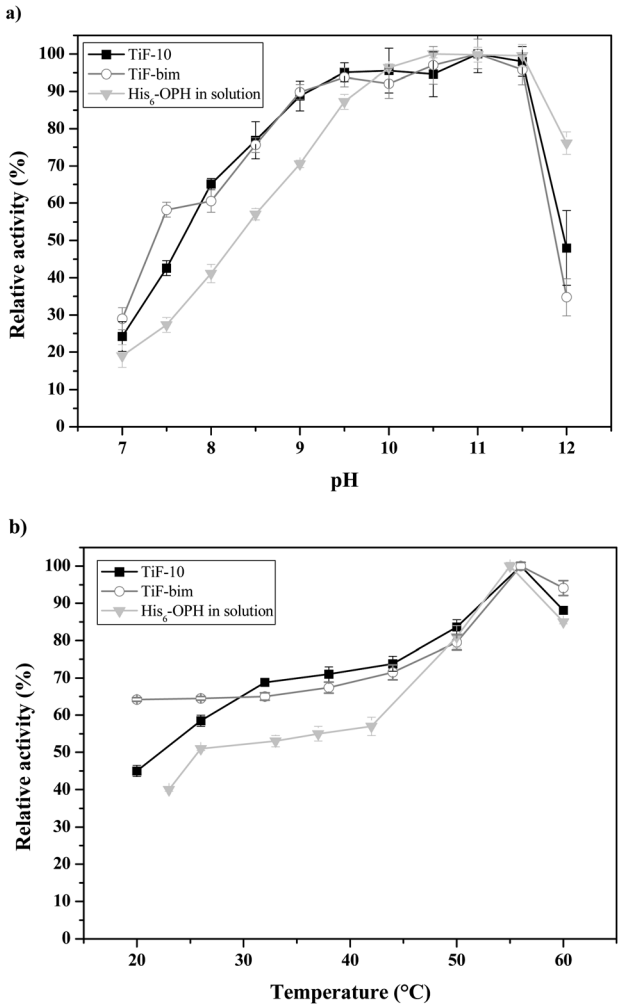

Fig. 4 Influences of (a) pH and (b) temperature on the activities of the biocatalyst thin films TiF-10 (filled squares) and TiF-bim (empty circles) and His_6–OPH in solution (filled triangles). Measurements were performed with selected 50 mm^2 bio-functionalized mesoporous titania thin films with covalently attached His_6–OPH. Substrate: 0.3 mM paraoxon.

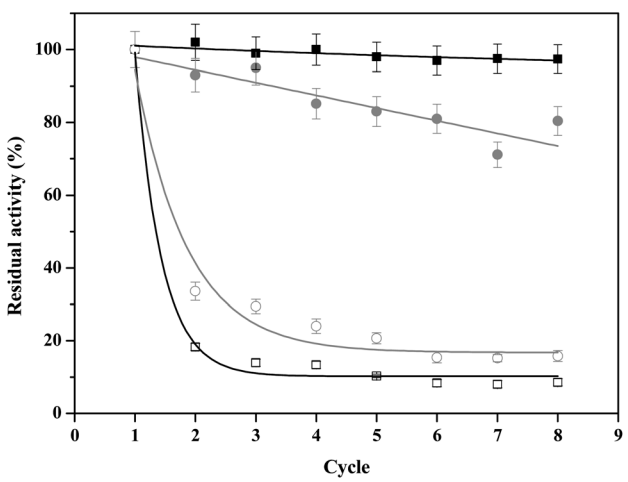

Fig. 5 Cycles of usage for covalently attached His_6–OPH, TiF-10 and TiF-bim (black and grey squares), and adsorbed His_6–OPH, TiF-10, TiF-10 and TiF-bim (black and grey circles). Measurements were performed with selected 50 mm^2 bio-functionalized mesoporous titania thin-films with covalently attached His_6–OPH at 20 °C and pH 10.5 (CB, 50 mM). Substrate: 0.3 mM paraoxon.

only, was also measured. A remarkable contrast is observed, as the catalytic performance of bio-functionalized mesoporous films obtained through adsorption deteriorates significantly on repeated use, losing more than 60% of the activity after the first cycle, and leveling off at a remaining activity of 10–20% after eight cycles. These data lead to a simple conclusion; the used enzyme is only adsorbed onto the surface of synthesized films and does not enter the pores, which are either too small or too large to successfully accommodate the enzyme and do not offer the desired environment for efficient immobilization. The low activity of adsorbed enzyme may also be due to interrupted physical forces that are the consequence of high pH where the charge of OPH, at which the measurements are performed (pH of 10.5; pI of OPH is at 8.5 (ref. 15)), changes and causes enzyme detachment. Furthermore, the biocatalyst films with adsorbed enzyme do not fulfill the desired requirement for repeatable use. This is in contrast with the observed stability after several cycles of adsorbed α-amilase[50] or DNA polymerase[52] in mesoporous films. It is possible that operating above the isoelectric point of the enzyme (His_6–OPH has a pI of 8.5 according to Votchitseva *et. al.*[15]) and titania leads to the detachment of the catalyst due to an unfavorable electrostatic interaction.

The stabilities of the titania-confined enzymes were investigated by measuring their activities several days after the biosensing film preparation. The biocatalyst films with covalently attached His_6–OPH were stored in closed vessels containing phosphate buffer (25 mM, pH 7.5) at 4 °C. The biocatalyst films' signal relative to day 1 is considered to be 100%. From the obtained data, it could be concluded that drastic drops in activity (~50%) take place around the 5th day after the films' preparation. After the 14th day, approximately 20% of the initial activity levels remain. Clearly, for sufficient usage the prepared biocatalyst films should be used within one week (Fig. 6).

Conclusions

Mesoporous titania thin films displaying either 9 nm diameter monodisperse pores or hierarchical structures with bimodal pore size distributions (13–38 nm pore diameter) were found to be a suitable material for an organophosphate hydrolase (His_6–OPH) immobilization. These inorganic matrices indeed permit an efficient enzyme operation while protecting it from external influences. The method presented here is straightforward, and permits the successful production of biocatalyst films with good activity and sensitivity down to 15 μM concentration for the selected substrate, in this case paraoxon. The immobilized enzyme possesses broadened pH and temperature working range. The biocatalyst films reveal an excellent activity at neutral pH and lower temperatures allowing them to be more properly applied in water analysis on OP compounds. Differences in the nature of used carriers are distinct; films with bimodal pore size distribution seem to be the better choice, owing to their 65% immobilization efficiency and 50% higher activity retention. Furthermore, the reusability of these biocatalyst films was proven to last at least for whole eight cycles; in the case of covalently attached enzymes, minimal or no losses in activity were observed. Our study permits to understand the different reactivity, performance and stability of the enzyme-mesoporous films, thus leading to the design of large-scale porous bioactive coatings for sensing with enhanced stability and reusability. To the best of our knowledge, no work in thin films with OPH has yet been published. It is worth to remark that the enzyme-mesoporous film platform presented here is flexible, as it permits to perform optical detection, and has the potential to be extended to electrochemical detection, by simply depositing the mesoporous film onto a conductive substrate.

The results obtained by applying biocatalyst thin films based on the covalent attachment of His_6–OPH on hierarchical mesoporous titania show great potential in the determination and detoxification of paraoxon. Presently, the conventional analysis of pesticide residues in agricultural commodities and water is a labor-intensive process, since it is necessary to cover a wide range of different chemicals, using a single and time consuming procedure. The presented approach, with minor alterations, is a suitable alternative for routine analysis within the μM to mM concentration range, as it allows for analytical data to be obtained within minutes and the instrumentation required is very simple and usually part of basic laboratory equipment. The limitation of our existing biocatalyst films lies in the sensitivity for the selected pesticide (paraoxon). One improvement could be accomplished through altering the existing detection technique. A further increase in the biocatalyst films' sensitivity could arise by increasing the concentrations of immobilized enzyme per mm^2 carrier, by enlarging the surface areas of used carriers, or by resorting to electrochemical detection.

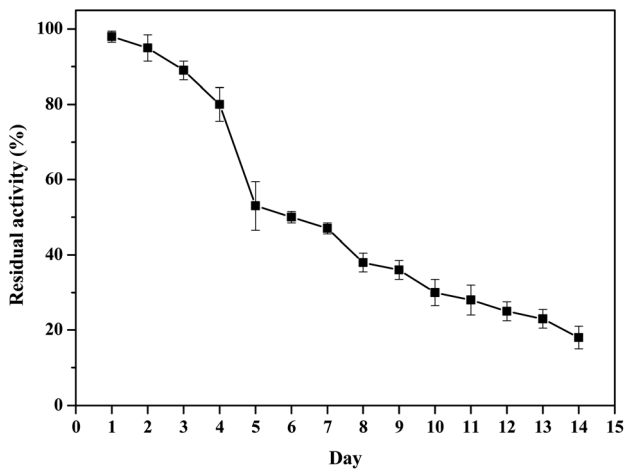

Fig. 6 Stability of the titania bio-sensing film (TiF-9) with covalently attached enzyme several days after the film preparation.

Acknowledgements

This work was supported by the grant from the Slovenian Research Agency (ARRS) for Young researchers (1000-08-310045) and by ANPCyT (PICT 2008-1848 and 2012-2087). Financial support for travel by N. Frančič from The University of Maribor to Comision Nacional de Energíá Atomica was

generously provided by the Slovene Human Resources Development and Scholarship Fund, Ad Futura funding of research collaboration for Slovene PhD students in foreign countries (11012-21/2009-4).

References

1 J. M. Woodley, *Trends Biotechnol.*, 2008, **26**, 321.
2 L. Que and W. B. Tolman, *Nature*, 2008, **455**, 333.
3 J. S. Dordick and A. Freeman, *Curr. Opin. Biotechnol.*, 2006, **17**, 559.
4 H. E. Schoemaker, D. Mink and M. G. Wubbolts, *Science*, 2003, **299**, 1694.
5 *Biomolecular Catalysis: Nanoscale Science and Technology: ACS Symposium Series, No. 986*, 2008.
6 L. Cao, *Carrier-Bound Immobilized Enzymes: Principles, Applications and Design*, Wiley-VCH, Weinheim, Germany, 2005.
7 J. Ma, L. Zhang, Z. Liang and Y. Zhang, *J. Sep. Sci.*, 2007, **30**, 3050.
8 P. Johnson and T. L. Whately, *J. Colloid Interface Sci.*, 1971, **37**, 557.
9 D. Avnir, S. Braun, O. Lev and M. Ottolenghi, *Chem. Mater.*, 1994, **6**, 1605.
10 M. T. Reetz, A. Zonta and J. Simpelkamp, *Angew. Chem., Int. Ed.*, 1995, **34**, 301.
11 D. Avnir, T. Coradin, O. Lev and J. Livage, *J. Mater. Chem.*, 2006, **16**, 1013.
12 E. Prouzet, S. Ravaine, C. Sanchez and R. Backov, *New J. Chem.*, 2008, **32**, 1284–1299.
13 J. E. Chambers and P. E. Levi, in: *Organophosphates: chemistry, fate, and effects*, Academic, New York, 1992, pp. 3–8.
14 E. N. Efremenko and V. S. Sergeeva, *Russ. Chem. Bull.*, 2001, **50**, 1825.
15 Y. A. Votchitseva, E. N. Efremenko, T. K. Aliev and S. D. Volfomeyev, *Biochemistry*, 2006, **71**, 167.
16 S. R. Caldwell and F. M. Raushel, *Appl. Biochem. Biotechnol.*, 1991, **31**, 59.
17 P. L. Havens and H. F. Rase, *Ind. Eng. Chem. Res.*, 1993, **32**, 2254.
18 K. E. LeJeune and A. J. Russell, *Biotechnol. Bioeng.*, 1996, **51**, 450.
19 K. E. LeJeune, A. J. Mesiano, S. B. Bower, J. K. Grimsley, J. R. Wild and A. J. Russell, *Biotechnol. Bioeng.*, 1997, **54**, 105.
20 K. E. LeJeune, J. S. Swers, A. D. Hetro, G. P. Donahey and A. J. Russell, *Biotechnol. Bioeng.*, 1999, **64**, 250.
21 V. A. Pedrosa, S. Paliwal, S. Balasubramanian, D. Nepal, V. Davis, J. Wild, E. Ramanculov and A. Simonian, *Colloids Surf., B*, 2010, **77**, 69.
22 P. B. Dennis, A. Y. Walker, M. B. Dickerson, D. L. Kaplan and R. R. Naik, *Biomacromolecules*, 2012, **13**, 2037.
23 C. Dosoretz, R. Armon, J. Starosvetzky and N. Rothschild, *J. Sol-Gel Sci. Technol.*, 1996, **7**, 7.
24 I. Gill and A. J. Ballesteros, *J. Am. Chem. Soc.*, 1998, **120**, 8587–8598.
25 A. K. Singh, A. W. Flounders, J. V. Volponi, C. S. Ashley, K. Wally and J. S. Schoeniger, *Biosens. Bioelectron.*, 1999, **14**, 703–713.
26 A. W. Flounders, A. K. Sigh, J. V. Volponi, S. C. Carincher, K. Wally, A. S. Simonian, J. R. Wild, J. S. Schoeniger, 1999, **14**, 715.
27 I. Gill and A. Ballesteros, *Biotechnol. Bioeng.*, 2000, **70**, 400–410.
28 H. Frenkel-Mullerad and D. Avnir, *J. Am. Chem. Soc.*, 2005, **127**, 8077.
29 N. Frančič, A. Košak, I. Lyagin, E. N. Efremenko and A. Lobnik, *Anal. Bioanal. Chem.*, 2011, **401**, 2631.
30 C. Lei, Y. Shin and E. J. Ackerman, *J. Am. Chem. Soc.*, 2002, **124**, 11242.
31 C. Lei, M. M. Valenta, K. P. Saripalli and E. J. Ackerman, *J. Environ. Qual.*, 2007, **36**, 233.
32 B. Chen, C. Lei, Y. Shin and J. Liu, *Biochem. Biophys. Res. Commun.*, 2009, **390**, 1177.
33 C. H. Lee, J. Lang, C. W. Yen, P. C. Shih, T. S. Lin and C. Y. Mou, *J. Phys. Chem. B*, 2005, **109**, 12277.
34 Y. Wang and F. Caruso, *Chem. Mater.*, 2005, **17**, 953.
35 M. Hartmann, *Chem. Mater.*, 2005, **17**, 4577.
36 H. H. P. Yiu and P. A. Wright, *J. Mater. Chem.*, 2005, **15**, 3690.
37 J. D. Bass, D. Grosso, C. Boissière, E. Belamie, T. Coradin and C. Sanchez, *Chem. Mater.*, 2007, **19**, 4349.
38 Y. T. Shi, R. Yuan, Y. Q. Chai, M. Y. Tang and X. L. He, *J. Electroanal. Chem.*, 2007, **604**, 9.
39 S. Liu and A. Chen, *Langmuir*, 2005, **21**, 8409.
40 Y. B. Xie, L. M. Zhou and H. T. Huang, *Biosens. Bioelectron.*, 2007, **22**, 2812.
41 L. Zhang, Q. Zhang, X. B. Lu and J. H. Li, *Biosens. Bioelectron.*, 2007, **23**, 102.
42 Y. H. Zhu, H. M. Cao, L. H. Tang, X. L. Yang and C. Z. Li, *Electrochim. Acta*, 2009, **54**, 2823.
43 R. A. Doong and H. M. Shih, *Biosens. Bioelectron.*, 2006, **22**, 185.
44 J. H. Yu, S. Q. Liu and H. X. Ju, *Biosens. Bioelectron.*, 2003, **19**, 401.
45 H. R. Luckarift, M. B. Dickerson, K. H. Sandhage and J. C. Spain, *Small*, 2006, **2**, 640.
46 J. Yu and H. Ju, *Anal. Chem.*, 2002, **74**(14), 3579.
47 F. Gao, P. Botella, A. Corma, J. Blesa and L. Dong, *J. Phys. Chem. B*, 2009, **113**, 1796.
48 S. M. Solberg and C. C. Landry, *J. Phys. Chem. B*, 2006, **110**, 15261.
49 S. Kataoka, A. Endo, M. Oyama and T. Ohmori, *Appl. Catal., A*, 2009, **359**, 108.
50 M. G. Bellino, A. E. Regazzoni and G. J. A. A. Soler-Illia, *ACS Appl. Mater. Interfaces*, 2009, **2**, 360.
51 L. Malfatti, M. G. Bellino, P. Innocenzi and G. J. A. A. Soler-Illia, *Chem. Mater.*, 2009, **21**, 2763.
52 M. G. Bellino, I. Tropper, H. Duran, A. E. Regazzoni and G. J. A. A. Soler-Illia, *Small*, 2010, **6**(11), 1221.
53 S. Mura, G. Greppi, A. M. Roggio, L. Malfatti and P. Inniocenzi, *Microporous Mesoporous Mater.*, 2011, **124**, 1.
54 E. Efremenko, Y. Votchitseva, F. Plieva, I. Galaev and B. Mattiasson, *Appl. Microbiol. Biotechnol.*, 2006, **70**, 558.

55 M. M. Bradford, *Anal. Biochem.*, 1976, **72**, 248.
56 N. C. Price, in: *Fundamentals of Enzymology: An Introduction to enzyme kinetics*, 3rd edn, Oxford University Press, 1999, pp. 118–153.
57 H. G. Tompkins and W. A. McGahan, in: *Spectroscopic Ellipsometry and Refractometry: A User's Guide*, John Wiley & Sons, New York, 1999.
58 C. Boissière, D. Grosso, S. Lepoutre, L. Nicole, A. Brunet-Bruneau and C. Sanchez, *Langmuir*, 2005, **21**, 12362.
59 N. Tokuriki, C. J. Jackson, L. Afriat-Jurnou, K. T. Wyganowski, R. Tang and D. S. Tawfik, *Nat. Commun.*, 2012, **3**, 1257.
60 P. Innocenzi, *J. Non-Cryst. Solids*, 2003, **316**, 309.
61 P. Falcaro, D. Grosso, H. Amenitsch and P. Innocenzi, *J. Phys. Chem. B*, 2004, **108**, 10942.
62 A. Barth and C. Zscherp, *Q. Rev. Biophys.*, 2002, **35**(4), 639.
63 A. Barth, *Biochim. Biophys. Acta, Bioenerg.*, 2007, **1767**(9), 1073.
64 M. Van de Weert, P. I. Haris, W. E. Hennink and D. J. A. Crommelin, *Anal. Biochem.*, 2005, **297**(2), 160.
65 W. Gerhartz, *General production methods, In Enzymes in industry: Production and applications*, New York, Wiley, John & Sons Publishers, 1990, vol. 67.
66 EU Water Framework Directive, http://europa.eu/environment/water/water-framework/index_en.html.
67 A. Ursoiu, C. Paul, T. Kurtán and F. Péter, *Molecules*, 2012, **17**, 13045.